

## A solution chemists view of surface chemistry

Paul W. Schindler  
Department of Inorganic Chemistry, University of Bern, 3012  
Bern, Switzerland

**Abstract** Reactions at oxide mineral - electrolyte interfaces such as adsorption of hydrogen ions, metal ions and anions as well as dissolution and nucleation are discussed in terms of a unified model which is based on reactions of surface hydroxyls  $\equiv\text{S-OH}$ , where  $\equiv\text{S}$  stands for the coordinatively undersaturated surface metal atoms. Adsorption of metal ions  $\text{M}^{2+}$  involves formation of surface complexes  $(\equiv\text{S-O})_n\text{M}^{(2-n)+}$  whereas adsorption of anions  $\text{L}^{1-}$  is based on ligand exchange to form  $(\equiv\text{S})_n\text{L}^{(n+1)-}$ . Co-adsorption of metal ions and anions results in the formation of ternary surface complexes. The existence of the proposed surface species is supported by EPR, ENDOR and EXAFS spectroscopy. The rate laws of proton- and ligand assisted dissolution of metal oxides can conveniently be expressed in terms of surface complexes. Heteronucleation requires the simultaneous adsorption of the components involved in the formation of the new solid phase.

### INTRODUCTION

Among the variety of surface reactions, the adsorption of metal ions and ligands from aqueous solution to oxide mineral surfaces have recently found some special interest. Such processes are thought to play a major role in the transport of both metal ions and ligands in the environments. The classical view of these processes is based on electrostatics. Minerals in aquatic environments exhibit a surface potential  $\Psi$  that is controlled by the concentrations of the so called potential determining ions in the aqueous phase. For oxides minerals  $\Psi$  is assumed to be controlled by hydrogen ions and thus by the pH of the aqueous solution. Negatively charged ligands are assumed to be adsorbed at positively charged surfaces formed at low pH values. The adsorption of metal ions is expected to require negatively charged surfaces that are formed at elevated pH values. Experimental observations were considered to be in agreement with these expectations although the pronounced difference in the adsorption behavior of metals ions such as  $\text{Pb}^{2+}$  (that exhibits strong affinity to oxide surfaces) and  $\text{Cd}^{2+}$  (that is only weakly bound) was not predictable from electrostatics. In 1972 James and Healy (ref. 1) noticed that  $\text{Co}^{2+}$  ions readily adsorb on positively charged  $\text{TiO}_2$  surfaces. This observation gave rise to a change in our perception of the above specified adsorption processes. The essence of this new paradigm is the surface complexation model that has been developed by Werner Stumm and the present author (ref. 2) and extended by many researchers such as James A. Davis (ref. 3), François M. M. Morel (ref. 4) and John C. Westall (ref. 5). The present paper gives a personal account of this development. Special emphasis will be placed on correlations between surface reactions and reactions in solution.

### THE CONCEPT

In the course of a study on the adsorption of metal ions at amorphous silica (ref. 6) and  $\text{TiO}_2$  (ref. 7) we noticed that plots (% adsorbed vs  $\log [\text{H}^+]$ , Fig. 1a) of our data showed essentially the same shape as the (% extracted vs  $\log [\text{H}^+]$ , Fig. 1b) curves observed in solvent extraction.

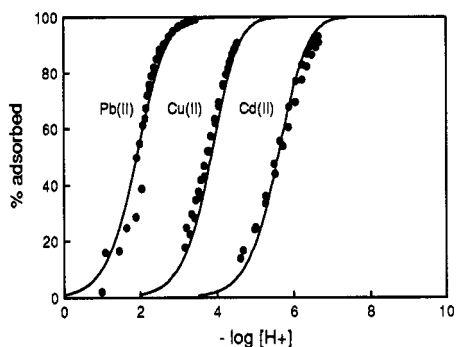


Fig. 1a. Adsorption of Pb(II), Cu(II) and Cd(II) from aqueous solution to  $\text{TiO}_2$  (rutile, ref. 7). The solid lines are model curves.

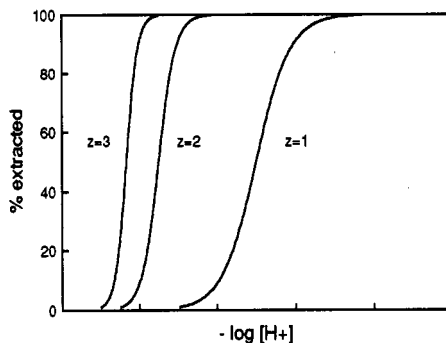
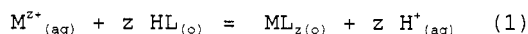
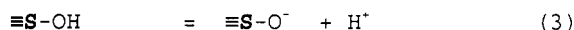
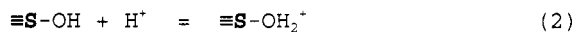


Fig 1b. Theoretical solvent extraction curves. Reproduced by permission from Morrison and Freiser (8).

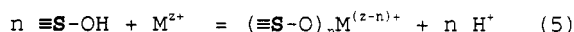
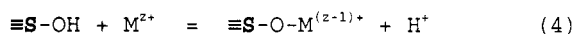
For the case of solvent extraction the sigmoid type curves reflect the equilibria



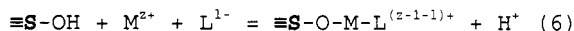
where the indices (aq) and (o) refer to aqueous and organic phases respectively. In search of a surface ligand which acts like the dissolved ligand HL in solvent extraction we recalled the early work of Hair (ref. 9) and Peri (ref. 10) which presents ample evidence for oxide and hydroxide surfaces being covered with surface hydroxyl groups. Similarly, sulfide surfaces seem to contain surface SH groups. For the subsequent discussion surface hydroxyls will be symbolized by  $\equiv\text{S-OH}$ , where  $\equiv\text{S}$  stands for the coordinatively undersaturated surface metal atoms. The chemistry of these surface hydroxyl groups can be characterized as follows (ref. 11): The presence of two lone electron pairs and a dissociable hydrogen indicates that these groups are potential ampholytes. It is thus reasonable to assume that surface hydroxyls can both accept and release a proton:



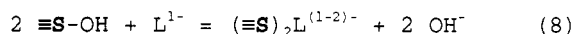
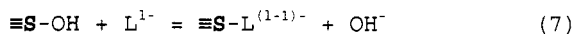
Deprotonated surface hydroxyls exhibit Lewis base behavior. Adsorption of metal ions is thus understood as complex formation involving one or several surface hydroxyls:



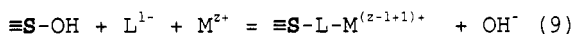
The hitherto published studies seem to indicate that  $n$  does not exceed a value of 2. Since the coordination sphere of the adsorbed metal is thus only partially occupied by the surface ligands, additional ligands L from the solution may be acquired:



The surface species formed in reaction (6) is called a type A ternary surface complex. Although the formation of type A ternary surface complexes leads to adsorption of anions (ligands), the principal mechanism of anion (ligand) adsorption is based on ligand exchange. Again one or two surface hydroxyls may be involved:



In cases where L is a polydentate ligand anchoring at the surface with one or two ligand atoms, further ligand atoms may be used to bind metal ions from solution:



The species formed in the reaction (9) is a type B ternary surface complex.

### FORMULATING EQUILIBRIUM CONSTANTS

Let us consider the simple equilibrium (4). The intrinsic microscopic equilibrium constant is defined by the equation

$$K^e_{(int)} = a_{\equiv\text{SOM}} a_{\text{H}} / a_{\equiv\text{SOH}} a_{\text{M}} \quad (10)$$

where  $a_i$  denotes the activity of the surface species  $i$ . For convenience this activity will be expressed as the product of the surface concentration  $\{i\}$  (in mol per kg of adsorbing solid) and the surface activity coefficient  $\gamma_i$  (in  $\text{kg mol}^{-1}$ ):

$$K^e_{(int)} = \{\equiv\text{SOM}\} \gamma_{\equiv\text{SOM}} a_{\text{H}} / \{\equiv\text{SOH}\} \gamma_{\equiv\text{SOH}} a_{\text{M}} \quad (10a)$$

It is possible to measure the surface concentrations  $\{\equiv\text{SOH}\}$  and  $\{\equiv\text{SOM}\}$ . It is sometimes convenient to express the concentrations of the surface species in the same units as the concentrations of the solutes ( $\text{mol dm}^{-3}$ ). This conversion can be performed by the equation

$$\{\equiv\text{SOH}\} = (A/V) \{\equiv\text{SOH}\} \quad (11)$$

where  $A$  is the mass of suspended solid mineral (kg) and  $V$  is the volume of the solution ( $\text{dm}^3$ ). It is, unfortunately, in most cases not possible to experimentally evaluate the surface activities  $a_{\text{H}}$  and  $a_{\text{M}}$ , respectively. At equilibrium, the electrochemical potentials of  $\text{H}^+$  and  $\text{M}^{z+}$  are equal in both phases:

$$\mu^*_{(\text{H}, \text{aq})} = \mu^*_{(\text{H}, \text{surf})} ; \mu^*_{(\text{M}, \text{aq})} = \mu^*_{(\text{M}, \text{surf})} \quad (12)$$

The electrochemical potential of a species  $i$  in a phase  $j$  is given by

$$\mu^*_{(i, j)} = \mu^{\circ}_{(i, j)} + RT \ln a_{(i, j)} + z_i F \Psi_{(j)} \quad (13)$$

where  $\Psi_{(j)}$  is the potential at phase  $j$ ,  $z_i$  is the charge number of the species  $i$  and  $\mu^{\circ}_{(i, j)}$  is the standard potential. In the presence of an ionic medium of constant ionic strength, the activities of solute species can, without any loss of rigor, be replaced by concentrations. By choosing the standard states to be the same in both phases

$$\mu^{\circ}_{(\text{H}, \text{aq})} = \mu^{\circ}_{(\text{H}, \text{surf})} ; \mu^{\circ}_{(\text{M}, \text{aq})} = \mu^{\circ}_{(\text{M}, \text{surf})} \quad (14)$$

and by assigning a zero potential to the aqueous solution, we obtain

$$\begin{aligned} a_{\text{H}} &= [\text{H}^+] \exp(-F\Psi/RT) ; \\ a_{\text{M}} &= [\text{M}^{z+}] \exp(-zF\Psi/RT) \end{aligned} \quad (15)$$

Combining (10a) and (15) results in

$$K^e = K^e_{(int)} \Gamma \quad (16)$$

where

$$K^e = \{\equiv\text{SOM}\} [\text{H}^+] / \{\equiv\text{SOH}\} [\text{M}^{z+}] \quad (17)$$

is the experimentally accessible conditional stability constant and

$$\Gamma = (\gamma_{\text{SOM}}/\gamma_{\text{SOH}}) \exp((z-1)\Psi/RT) \quad (18)$$

collects terms that contribute to deviation from ideality.

### NUMERICAL IMPLEMENTATION

The previous section leaves us with the problem of evaluating intrinsic stability constants from the experimentally accessible conditional constants. Any solution of this problem requires awareness of the physical nature of the factors that are responsible for the non-ideal behavior. These factors are: a) The above mentioned surface potentials that originate from the adsorption of charged species. Note that in this paper the concept of potential determining ions is used in an extended sense as to include every kind of adsorbed ions. For the simple case that only one charged species is adsorbed, the surface potential will vanish at zero surface coverage. For the case of

simultaneous adsorption of various charged species, the surface potential will again vanish at zero surface coverage and in addition at conditions where the charges of the adsorbed species compensate each other.

b) Lateral interactions (both attraction and repulsion) based on coulombic and van der Waals forces. Again these lateral interactions will vanish at zero surface coverage.

c) Surface heterogeneity i. e. the presence of  $\equiv\text{S-OH}$  groups with different binding properties that is in turn reflected by different  $K^{\text{s}}_{(\text{int})}$  values. At low surface coverage, adsorption will be based on reaction with surface hydroxyls with maximum  $K^{\text{s}}_{(\text{int})}$  values.

With charged species there is a strong overlap of the first two factors, and the above mentioned separation of  $\Gamma$  into terms comprising surface potentials and activity coefficients, respectively, is not unambiguous.

### Studies at low surface coverage

From the above considerations it becomes evident that the effect of both surface potentials and lateral interactions and thus the difference between  $K^{\text{s}}$  and  $K^{\text{s}}_{(\text{int})}$  decrease with decreasing surface coverage and may eventually escape experimental observation. Hence the above (Fig. 1a) shown data on trace adsorption of Pb(II), Cu(II) and Cd(II) on  $\text{TiO}_2$  were modelled with the aid of conditional constants.

### Extrapolation techniques

In favorable cases where adsorption can be described by just one reaction leading to a single surface complex i, the intrinsic stability constant can be obtained from extrapolation of  $K^{\text{s}}$  values obtained at various surface coverages to zero coverage or zero charge conditions. This extrapolation is greatly facilitated in cases where  $K^{\text{s}}$  and  $K^{\text{s}}_{(\text{int})}$  are related by a Frumkin type equation

$$K^{\text{s}} = K^{\text{s}}_{(\text{int})} \exp(\alpha[i]) \quad (19)$$

$$\log K^{\text{s}} = \log K^{\text{s}}_{(\text{int})} + (\alpha/\ln(10))[i] \quad (20)$$

and  $\log K^{\text{s}}$  is a linear function of  $[i]$ , the concentration of the surface complex i. Details of the extrapolation technique are given by Schindler and Stumm (ref. 2).

### Double layer techniques

By double layer techniques we will designate the various methods used to evaluate  $K^{\text{s}}_{(\text{int})}$  on the basis of equations (16) and (18) using different models (namely the constant capacitance model (ref. 12), the Gouy - Chapman model, the Stern model and the triple layer model (ref. 13)) of the electrified water mineral interface. For a detailed account of the different models the reader is referred to Bolt and Van Riemsdijk (ref. 14) and to Davis and Kent (ref. 3). The models have in common that they neglect lateral interactions assuming, therefore, unit surface activity coefficients. They are furthermore presumed to be equivalent in fitting the experimental data (ref. 15) although this conclusion was drawn from a rather limited set of experimental data. They differ in their perception on how the Gibbs free energy of adsorption

$$\Delta G_{(\text{ads})} = - RT \ln(10) \log K^{\text{s}} \quad (21)$$

is split into

$$\Delta G_{(\text{int})} = - RT \ln(10) \log K^{\text{s}}_{(\text{int})} \quad (22)$$

and

$$\Delta G_{(\text{coul})} = zF\Psi \quad (23)$$

They differ, moreover, in the number of adjustable parameters. Whereas the Gouy-Chapman models does not require any adjustable parameter, both the constant capacitance and the Stern model contain a specific capacitance as an adjustable variable. The triple layer model requires values for both the inner and the outer Helmholtz capacitance. Therefore, the different models produce somewhat different values of  $K^{\text{s}}_{(\text{int})}$  and sometimes even different surface species. Despite of these complications, the use of double layer techniques is strongly indicated for elucidating adsorption processes involving several simultaneous reactions. Westall's (ref. 16) FITEQL is an almost ideal computer program for evaluating intrinsic stability constants of simultaneously occurring surface reactions.

**CORRELATIONS BETWEEN SURFACE COMPLEXATION AND COMPLEX FORMATION IN SOLUTION**

The above mentioned techniques have widely been used to produce stability constants of surface complexes. Selected values are given by Dzombak and Morel (ref. 4 ) and by Schindler and Sposito (ref. 11 ). Instead of just presenting an updated collection of selected values we shall focus our interests to correlations between the stabilities of surface complexes and related complexes in solution. The basis of these correlations is given in Table 1.

TABLE 1. Surface reactions and related reactions in solution

Surface reaction	Reaction in solution
a) Acid-base reactions	
$\equiv\text{S-OH}_2^+ = \equiv\text{S-OH} + \text{H}^+ \quad K_a^s$	$\text{M(OH)}_{(z-1)}^+ + \text{H}_2\text{O} = \text{M(OH)}_z^+ + \text{H}^+ \quad {}^*K_z$
$\equiv\text{S-OH} = \equiv\text{S-O}^- + \text{H}^+ \quad K_a^s$	$\text{M(OH)}_z^0 + \text{H}_2\text{O} = \text{M(OH)}_{(z+1)}^- + \text{H}^+ \quad {}^*K_{(z+1)}$
b) Adsorption of metal ions	
$\equiv\text{S-OH} + \text{M}^{z+} =$	$\text{H-OH} + \text{M}^{z+} =$
$\equiv\text{S-OM}^{(z-1)*} + \text{H}^+ \quad {}^*K_1^s$	$\text{H-OM}^{(z-2)} + \text{H}^+ \quad {}^*K_1$
$2 \equiv\text{S-OH} + \text{M}^{z+} =$	$2 \text{H-OH} + \text{M}^{z+} =$
$(\equiv\text{S-O})_2 + 2 \text{H}^+ \quad {}^*\beta_2^s$	$(\text{HO})_2\text{M}^{(z-2)+} + 2 \text{H}^+ \quad {}^*\beta_2$
c) Adsorption of ligands	
$\equiv\text{S-OH} + \text{HL} =$	$\text{M-OH}_{(z-1)}^1 + \text{HL} =$
$\equiv\text{S-L} + \text{H}_2\text{O}$	$K_1^s \quad \text{ML}^{(z-1)+} + \text{H}_2\text{O} \quad K_1$

For a rigorous comparison, statistical factors should be included, since surface stability constants are microscopic constants whereas  ${}^*K$  values in solutions reflect macroscopic constants. Fig. 2 compares acidity constants of  $\equiv\text{S-OH}$  groups with acidity constants of related hydroxo complexes in solution. The data suggests the correlation

$$\log K_{a(\text{int})}^s = -2.43 + 0.7 \log {}^*K$$

Stability constants of hydroxo complexes correlate also with surface stability constants of metal complexes. Fig. 3 shows the excellent correlation for

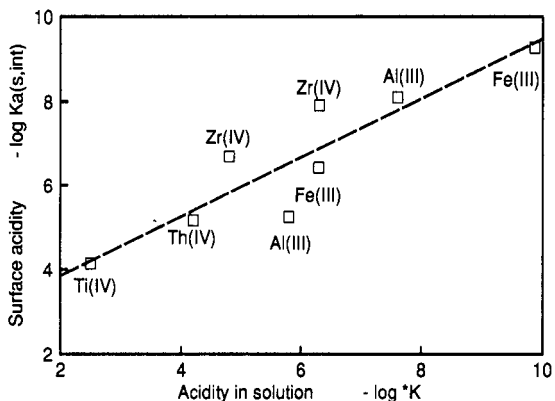


Fig. 2. Correlation of surface acidity constants (ref. 11) and stability constants of hydroxo complexes in solution ( ref. 17).

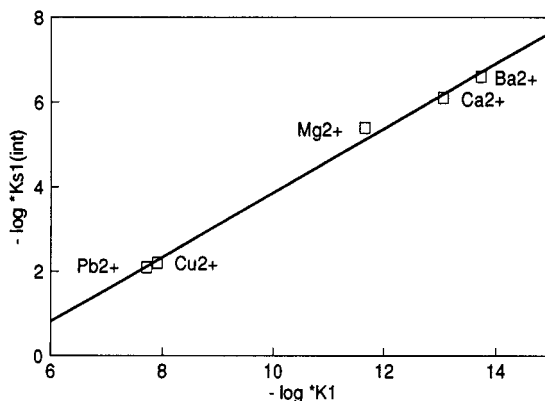


Fig. 3. Correlation of surface stability constants of metal complexes (ref. 11) at  $\gamma\text{-Al}_2\text{O}_3$  and stability constants of hydroxo complexes in solution. The solid line corresponds to the equation  $\log {}^*K_{1(\text{int})}^s = 3.75 + 0.76 \log {}^*K_1$ .

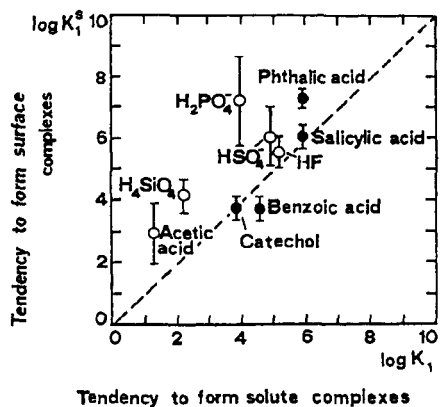


Fig. 4.

Correlation of stability constants of anion complexes at  $\alpha$ -FeOOH (empty circles) and  $\gamma$ -Al<sub>2</sub>O<sub>3</sub> (full circles) with stability constants of dissolved species. Reproduced by permission from Stumm et al. (ref. 18).

surface complexes at  $\gamma$ -Al<sub>2</sub>O<sub>3</sub>. Similar correlations have been found for amorphous silica (ref. 6) and amorphous Fe(III) hydroxide (ref. 4).

Finally ligand exchange involving  $\equiv$ S-OH groups correlates fairly well with ligand exchange equilibria of monohydroxo complexes in solution (Fig. 4). On the basis of the known stabilities of hydroxo species in solution one can thus get estimates of unknown surface stability constants. Moreover, the observed correlations give some support for the assumption of surface species being true inner sphere complexes.

#### SUPPORT FROM SPECTROSCOPY

Further evidence for surface coordination has been provided by ESP and UV - visible spectroscopy of Cu<sup>2+</sup> adsorbed at aluminium hydroxides (refs. 19 - 21). These spectra are different from those of Cu(H<sub>2</sub>O)<sub>6</sub><sup>2+</sup>, suggesting that the surface oxygens have displaced one or two water molecules in the inner hydration sphere of Cu<sup>2+</sup>. Spectroscopic evidence for a similar mechanism of VO<sub>2</sub><sup>+</sup> coordination to alumina surfaces has been reported (refs. 20, 22). The most direct insight into the coordinative environment of adsorbed metal ions and anions is offered by EXAFS and XANES spectroscopy. The structural information is not limited to the first shell but extends to second-, and third-nearest neighbors. Studies of Pb(II) on  $\gamma$ -Al<sub>2</sub>O<sub>3</sub> (refs. 23, 24) reveal the presence of one second neighbor Al and one second neighbor Pb atom. The observed Pb-O and Pb-Al distances are consistent with the formation of the monodentate mononuclear complexes  $\equiv$ Al-OPb<sup>+</sup> and  $\equiv$ Al-OPb(OH)<sup>0</sup>. The presence of a second neighbor Pb is a consequence of the comparatively high surface density and can be attributed to the presence of a small fraction of multinuclear complexes. A study of Pb(II) on  $\alpha$ -FeOOH at 15% surface coverage (ref. 25) again showed the presence of monomeric inner sphere complexes. The results of similar studies of Co<sup>2+</sup> on  $\gamma$ -Al<sub>2</sub>O<sub>3</sub>, TiO<sub>2</sub>, kaolinite and quartz (refs. 24, 26,) can be summarized as follows: At low surface coverage mononuclear inner-sphere complexes are formed. With increasing surface coverage multinuclear adsorption complexes of increasing size as saturation is approached are formed. A three-dimensional hydroxide phase is formed in systems where the solubility product of Co(OH)<sub>2</sub> is exceeded. For details the reader is referred to the recent review by Brown (ref. 27).

#### CONCLUSIONS AND APPLICATIONS

Looking at oxide mineral - water interfaces from the point of view of solution chemistry offers a consistent and convenient way for describing adsorption equilibria. Adsorption of H<sup>+</sup>, OH<sup>-</sup>, metal ions and anions can now be handled the same way as solution equilibria. This unification was found to be useful in computers programs for modeling soil solutions and other natural aquatic systems (refs. 28, 29). In addition, the surface complexation model offers a key for understanding dissolution and nucleation reactions.

#### Proton assisted dissolution

The rate of dissolution of oxides is known to increase with increasing hydrogen ion concentration. In many cases the observed reaction order with respect to H<sup>+</sup> is, however, a non-integer number. For instance, the dissolution of BeO in HCl was found to follow the rate law

$$d[\text{Be}^{2+}]/dt = k[\text{H}^+]^{0.5}$$

Furrer and Stumm (ref. 30) have shown that reaction orders corresponding to integer numbers are obtained if the reaction rates are related to the surface concentrations  $c_H^s$  of  $H^+$ , i.e. the concentrations of protonated surface hydroxyls:



The underlying mechanism is thought to consist of two (BeO) or three ( $\text{Al}_2\text{O}_3$ ) fast protonation steps followed by the rate determining detachment step.

#### Ligand assisted and proton-ligand assisted dissolution

Furrer and Stumm (ref. 30) have studied the dissolution of BeO,  $\delta\text{-Al}_2\text{O}_3$  and Fe(III)-oxides in the presence of bidentate ligands L (L: oxalate, malonate, succinate, salicylate, phthalate). The rate  $R_{L,H}$  of dissolution was found to follow the law:

$$R_{L,H} = k_L c_L^s (c_H^s)^n$$

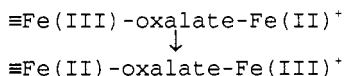
where  $c_L^s$  is the surface concentration of the adsorbed ligand in the specific form of a surface chelate and  $n$  is an integer usually equal to zero. With dicarbonic acids the sequence

$$k_{\text{oxalate}} < k_{\text{malonate}} < k_{\text{succinate}}$$

was observed indicating that oxalate that forms a five membered ring causes the most rapid dissolution. The effect of ring size was also observed with aromatic ligands.

#### Reductive dissolution

Changes in the oxidation state are coupled with changes in both solubility and dissolution rates. Reduction of Fe(III) to Fe(II) not only increases the solubility of the corresponding oxide but also increases the rate of dissolution. Hence the rate of dissolution of Fe(III) is usually greatly enhanced by the presence of a reductant. The accelerating effect is, however, only observed under conditions where the reductant is adsorbed. Hence, the reductive dissolution of  $\text{Fe}_2\text{O}_3$  by  $\text{Cr}^{2+}$  (ref. 31) is probably based on the formation of a type B ternary surface complex  $\equiv\text{Fe(III)-Cl-Cr(II)}^{2+}$  followed by electron transfer and rapid dissolution of the formed Fe(II) surface site (ref. 32). Recent work on the reductive dissolution of magnetite (ref. 33),  $\alpha\text{-FeOOH}$  (ref. 34) and  $\alpha\text{-Fe}_2\text{O}_3$  (refs. 35-37) have revealed the key role of the complexes



in the reductive dissolution of iron minerals by oxalic acid.

#### Adsorption and nucleation

Hohl et al. (ref. 38) have investigated the heteronucleation of  $\text{CaF}_2$  on  $\text{CeO}_2$ . In the course of these investigations a series of oversaturated  $\text{CaF}_2$  solutions were prepared and reacted with  $\text{CeO}_2$  seeds. Surprisingly, the range of nucleation was restricted to the range where both  $\text{Ca}^{2+}$  and  $\text{F}^-$  are adsorbed. The rate of nucleation was found to follow the equation

$$R = c_{\text{Ca}}^s (c_{\text{F}}^s)^2$$

where  $c_{\text{Ca}}^s$  and  $c_{\text{F}}^s$  are the surface concentrations of adsorbed  $\text{Ca}^{2+}$  and  $\text{F}^-$  respectively.

**Acknowledgement** The research of surface complexation has been supported by the Swiss National Science Foundation.

#### REFERENCES

1. R.O. James and Th.W. Healy, *J. Colloid Interface Sci.*, **40**, 42-52 (1972).
2. P.W. Schindler and W. Stumm, *Aquatic Surface Chemistry*, W. Stumm (ed.), pp. 83-110, Wiley, New York (1987).

3. J.A. Davis and D.B. Kent, Mineral-Water Interface Geochemistry, M.F. Hochella Jr. and A.F. White (eds.), pp. 177-260, Mineralogical Society of America, Washington D.C. (1990).
4. D.A. Dzombak and F.M.M. Morel, Surface Complexation Modeling, Wiley, New York (1990).
5. J.C. Westall, Aquatic Surface Chemistry, W. Stumm (ed.), pp. 3-32, Wiley, New York (1987).
6. P.W. Schindler, B. Fürst, R. Dick and P.U. Wolf, J. Colloid Interface Sci., **55**, 469-475 (1976).
7. B. Fürst, Das koordinationschemische Adsorptionsmodell: Oberflächenkomplexbildung von Cu(II), Cd(II) und Pb(II) an SiO<sub>2</sub> (Aerosil) und TiO<sub>2</sub> (Rutil), Ph.D. Thesis, Bern (1976).
8. G.H. Morrison and H.F. Freiser, Solvent Extraction in Analytical Chemistry, p.56, Wiley New York (1957).
9. M.L. Hair, Infrared Spectroscopy in Surface Chemistry, Dekker, New York (1967).
10. J.B. Peri, J. Phys. Chemistry, **69**, 220-230 (1965).
11. P.W. Schindler and G. Sposito, Interactions at the Soil Colloid - Soil Solution Interface, H. Bolt, M.F. De Boot, M.H.B. Hayes, M.B. McBride (eds.), pp. 115-145, Kluwer, Dordrecht (1991).
12. P.W. Schindler and H. Gamsjäger, Kolloid Z. Polymere, **250** 759-763 (1972).
13. J.A. Davis, R.O. James and J.O. Leckie, J. Colloid Interface Sci., **63**, 480-499 (1978).
14. G.H. Bolt and W.H. Van Riemsdijk, Interactions at the Soil Colloid - Soil Solution Interface, G.H. Bolt, F. de Boot, M.H.B. Hayes, M.B. McBride eds.), pp. 37-79, Dordrecht (1991).
15. J.C. Westall and H. Hohl, Adv. Colloid Interface Sci., **12**, 265-293 (1980).
16. J.C. Westall, FITEOL Version 2.0, Report 82-02, Dept. of Chemistry, Oregon State Univ., Corvallis, Oregon (1982).
17. Ch.F. Baes Jr. and R.E. Mesmer, The Hydrolysis of Cations, Wiley, New York (1976).
18. W. Stumm, R. Kummert and L. Sigg, Croat. Chem. Acta, **53**, 291-312 (1980).
19. G. Martini, V. Bassetti and M.F. Ottaviani, Journal de Chimie Physique, **77**, 311-317, (1980).
20. M. Rudin and H. Motschi, J. Colloid Interface Sci., **98**, 385-393 (1984).
21. M.B. McBride, Soil Sci. Soc. Amer. J., **49**, 843-846 (1985).
22. M.B. McBride, J. Colloid Interface Sci., **120**, 419-429 (1987).
23. C.J. Chisholm-Brause, G.E. Brown Jr. and G.A. Parks, Physica, **B 158**, 646-648 (1989).
24. C.J. Chisholm-Brause, K.F. Hayes, A.L. Roe, G.E. Brown Jr. and G.A. Parks, Geochim. Cosmochim. Acta, **54**, 1897-1909 (1990).
25. A.L. Roe, K.F. Hayes, C.J. Chisholm-Brause, G.E. Brown Jr., G.A. Parks, K.O. Hodgson and J.O. Leckie, Langmuir, **7**, 367-373 (1991).
26. P.A. O'Day, C.J. Chisholm-Brause, G.E. Brown Jr. and G.A. Parks, EOS Trans. Am. Geophys. Union, **69**, 1482 (1988).
27. G.E. Brown, Mineral-Water Interface Geochemistry, M.F. Hochella Jr. and A.F. White (eds.), pp. 309 -363, Mineralogical Society of America, Washington D.C., (1990).
28. J.C. Westall, J.L. Zachary and F.M.M. Morel, MINEOL: A computer Program for the calculation of chemical equilibrium composition of aqueous systems. Tech. Note 18, Dept. Civil Eng., MIT, Cambridge (1976).
29. D.S. Brown and J.D. Allison, MINTEQA1. Equilibrium metal speciation model. A user's manual. EPA 600/3-87/012, U.S. Environmental Protection Agency, Athens (1987).
30. G. Furrer and W. Stumm, Geochim. Cosmochim. Acta, **50**, 1847-1860, (1986).
31. B.A. Zabin and H. Taube, Inorg. Chem., **3**, 963-968 (1965).
32. P.W. Schindler, Oester. Chem. Z., **86**, 141-147 (1985).
33. E. Baumgartner, M.A. Blesa, H.A. Marinovitch and A.J.G. Maroto, Inorg. Chem., **22**, 2224-2226 (1983).
34. R.M. Cornell and P.W. Schindler, Clays Clay Minerals, **35**, 347-352 (1987).
35. D. Suter, C. Siffert, B. Sulzberger and W. Stumm, Naturwissenschaften, **75**, 571-573 (1988).
36. S. Banwart, S. Davies and W. Stumm, Coll. Surf., **39**, 303-309 (1989).
37. J.G. Hering and W. Stumm, Mineral-Water Interface Geochemistry, M.F. Hochella Jr. and A.F. White (eds.), pp. 427-465, Mineralogical Society of America, Washington (1990).
38. H. Hohl, E. Werth, R. Giovanoli and E. Porsch, unpublished report as quoted in ref. 32.